Sequence Distribution and Its Effect on Glass Transition Temperatures of Poly(anhydride-*co*-imides) Containing Asymmetric Monomers

Andrea Staubli, Edith Mathiowitz,[†] and Robert Langer*

Department of Chemical Engineering, Massachusetts Institute of Technology, Cambridge, Massachusetts 02139

Received May 31, 1990; Revised Manuscript Received September 24, 1990

ABSTRACT: An ^{1}H NMR analysis was performed on poly(anhydride-*co*-imides)—containing both symmetric and asymmetric monomer units of varying degrees of hydrophobicity. The different diad sequences and their distribution throughout the polymer chain were determined from the relative intensities of the distinct proton signals for each diad. The obtained results were in all cases in close agreement with a Bernoullian distribution. Subsequent analysis of the glass transition temperatures (as a function of monomer structure and sequence distribution) showed that copolymers containing compatible monomers displayed a linear relationship between glass transition temperature and monomer fraction. On the other hand, copolymers containing monomers differing in size and chemical nature showed a negative deviation from linearity of their glass transition temperatures as a function of monomer fraction. The observed negative deviation from linearity in the latter case was successfully predicted by using theoretical models that take into account the sequence distribution of the monomer units and the effect of their compatibility and energetic interactions.

Introduction

The synthesis of a new class of erodible polymers containing amino acids integrated into the polymer backbone via hydrolytically labile anhydride bonds [e.g., the poly(anhydride-*co*-imides)] has been described recently.[1] Briefly, the imide-containing diacids were obtained through direct fusion of a mixture of anhydride and free amino acid, immobilizing the amine terminal of the amino acids in a cyclic imide structure. These dicarboxylic acid monomers were then converted to their mixed anhydrides with acetic acid and subsequently polymerized as either homo- or copolymers. An in-depth characterization of these polymers is described elsewhere.[2] This polymer class is characterized by an unusual combination of a rigid imide ring structure, which is known to provide structural integrity, and hydrolytically labile anhydride bonds, which ensure the degradability of these polymers. Incorporation of amino acids (naturally occurring and others) creates a wide variety of polymers with different properties. Thus, identification of basic structure–property relationships at the molecular level is necessary to be able to design new polymers with desired material properties.

Molecular spectroscopy is an important tool for the analysis of chemical structure, morphology, orientation, and molecular dynamics of a polymer chain[3]—all of which have an effect on material properties. A special case are copolymer systems. The properties of a copolymer depend both on the chemical nature of the repeating units and on their arrangement within the polymer chain, which results in either block, random, or strictly alternating copolymers. With ^{1}H NMR spectroscopy the composition and sequence distribution of copolymers[3,4] as well as the copolymerization mechanism[5] may be identified and related to other physicochemical properties, such as the glass transition.

Polymer glass transition temperature—representing the molecular mobility of the polymer chains—is an important phenomenon that influences the material properties and potential applications of a given polymer. Various structural characteristics (e.g., chain stiffness and intermolecular forces) influence the glass transition temperatures. The mobility of polymer chains depends on the possibility of rotation around the backbone carbon–carbon bonds. This itself is determined by the structure of the monomer unit, including any substituent groups. In general, the more hindered the rotation (because of large substituent groups), the higher the glass transition temperature. However, the opposite is observed in the case of flexible side chains, such as alkyl groups, which act more like plasticizers and therefore lower the glass transition temperatures. Intermolecular forces may include ionic interactions and hydrogen bonding. Other controllable parameters include the molecular weight of the polymer as well as the reaction conditions of the polymer synthesis and the conditions under which the analysis was performed. In-depth reviews on the glassy state and the glass transition are reported in the literature.[6]

Copolymerization of monomers (the homopolymers of which display different glass transition temperatures) may result in random or alternating copolymers, which display one single glass transition temperature, or in block or graft copolymers, which may adapt two distinct glass transition temperatures. Furthermore, depending on the structural similarity of the two monomers (i.e., depending on the rotational barriers of an A–B linkage as compared to either an A–A or B–B linkage), a linear relationship or (positive or negative) deviations from ideality can be observed. Thus, much attention has been devoted to developing theoretical models relating the glass transition phenomenology to molecular structure. Originally, the glass transition temperatures of copolymers were described by simple additive relations,[7,8] based on free-volume theories,[8,12-14] thermodynamic theories,[7] or kinetic theories,[15] which did not take into consideration the sequence distribution of the monomer units and the effect of their compatibility on steric and energetic interactions. The free-volume theory developed by Fox and Flory[12] suggests that the glass transition occurs when the free or unoccupied volume of the material reaches a constant value and does not decrease further as the material is cooled below its T_g. A thermodynamic theory, proposed by Gibbs and DiMarzio,[7] is based on the change of configurational entropy of a material as a function of temperature. At equilibrium it

---

[†] New address: Section of Artificial Organs, Department of Biology & Medicine, Brown University, Providence, RI 02904.

0024-9297/91/2224-2291$02.50/0

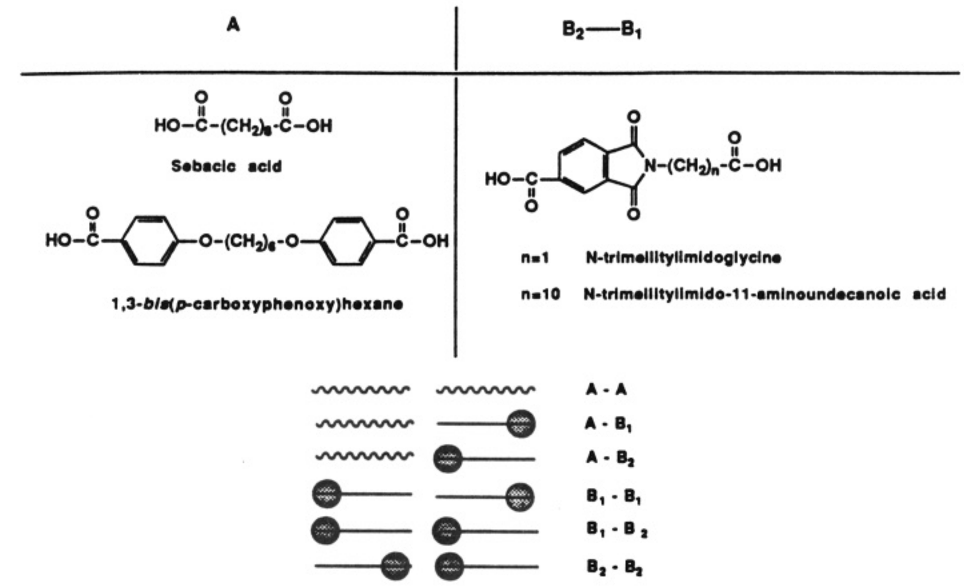

Figure 1. Monomer structures and schematic configuration of the six possible diad sequences in poly(anhydride-*co*-imides).

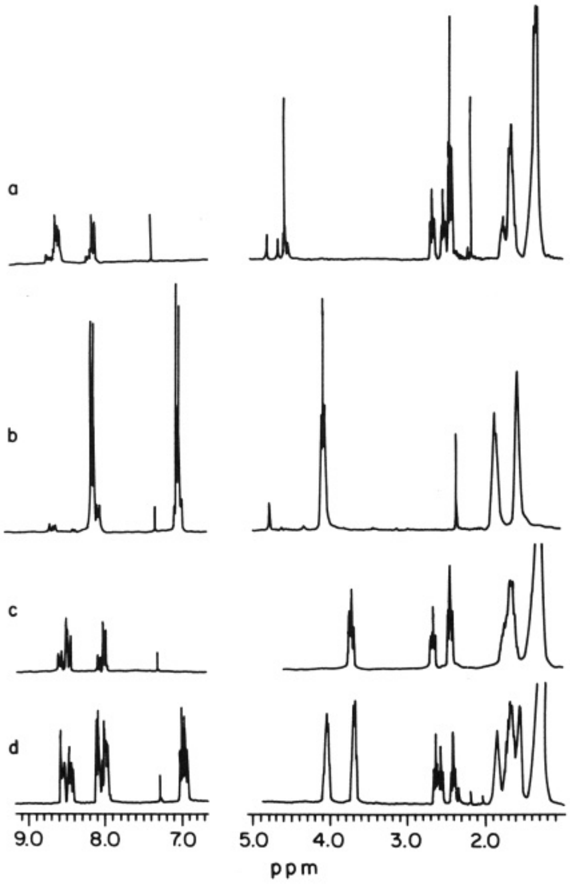

Figure 2. ^{1}H NMR spectra of (a) (TMA-gly:SA) (39:61), (b) (TMA-gly:CPH) (9:91), (c) (TMA-10:SA) (72:29), and (d) (TMA-10:CPH) (69:31).

Table I
Assignment of Proton Signals in ^{1}H NMR Spectra of (TMA-gly:SA) and (TMA-10:SA) Copolymers[a]

	(TMA-gly:SA)		(TMA-10:SA)	
diad	ppm	assgnmnt	ppm	assgnmnt
B_2–B_2	8.45–8.7	m, $H_{3',5'}$	8.55	s, $H_{3'}$ and d, $H_{5'}$
B_2–B_1 and B_2–SA	8.45–8.7	m, $H_{3',5'}$	8.45	s, $H_{3'}$ and d, $H_{5'}$
B_2–B_2	8.0–8.2	m, $H_{6'}$	8.05	d, $H_{6'}$
B_2–B_1 and B_2–SA	8.0–8.2	m, $H_{6'}$	7.95	d, $H_{6'}$
B $(CH_2)_{11}$			3.7	t, H_{11}
B_1–B_2	4.85	s, H_2	2.65	t, H_2
B_1–B_1	4.7	s, H_2	2.45	t, H_a
B_1–SA	4.6	s, H_2	2.45	t, H_a
SA–B_2	2.7	t, H_a	2.65	t, H_2
SA–*SA*	2.55	t, H_a	2.45	t, H_2
SA–B_1	2.4	t, H_a	2.45	t, H_2
B $(CH_2)_n$			1.6–1.8	m, $H_{3,10}$
SA $(CH_2)_n$	1.6–1.8	m, H_b	1.6–1.8	m, H_b
B $(CH_2)_n$			1.3	m, H_{4-9}
SA $(CH_2)_n$	1.3	m, H_c	1.3	m, H_c

[a] B_1 and B_2 represent the aliphatic and the aromatic ends, respectively, of the asymmetric imide-containing unit. The copolymer ratio was determined from the ratio of the integrated peak areas at 2.4–2.7 and 4.6–4.85 ppm in the case of (TMA-gly:SA) copolymers and 3.7 and 1.6–1.8 ppm in the case of (TMA-10:SA) copolymers, respectively (the italicized monomer represents the NMR-active one). TMA-*gly* possesses no more than one methylene group, which is reported separately for the various diads.

postulates that the configurational entropy, S_c, equals zero at glass formation. However, these linear relationships often failed in predicting accurate glass transition temperatures of copolymers, since they neglected the effect of the chemical nature and organization of the monomers on the mobility of a polymer chain.[10] Several models were therefore proposed[9–11] that differentiated between homo- (A–A, B–B) and heterolinkages (A–B), recognizing the significant effect of monomer arrangement on glass transition temperatures, such that both negative and positive deviations from linearity may be predicted. The relations proposed by Barton,[9] Uematsu and Honda,[16] Hirooka and Kato,[17] and Furukawa[18] may be considered as logical extensions of the Gibbs–DiMarzio relation,[7] whereas the approach by Johnston[10] is based on the Fox equation.[8] A third relation, developed by Couchman, is based on mixed-system entropy (expressed by glass transition temperatures and corresponding heat capacity increments)[11] and was also able to predict composition-dependent glass transition temperatures for a variety of systems, including miscible polymer blends and copolymers.[11] Furthermore, both the Barton and the Johnston relation could be obtained by nontrivial solutions of the theory proposed by Couchman. All of these relations have been successfully tested for a number of copolymer systems, showing both negative and positive deviations from linearity.

This report presents an in-depth characterization of selected poly(anhydride-*co*-imide) systems (Figure 1)—con-

Table II
Assignment of Proton Signals in ^{1}H NMR Spectra of (TMA-gly:CPH) and (TMA-10:CPH) Copolymers[a]

	(TMA-gly:CPH)		(TMA-10:CPH)	
diads	ppm	assgnmnt	peak	assgnmnt
B_2–B_2 and B_2–CPH	8.45–8.7	m, $H_{3',5'}$	8.65	s, $H_{3'}$ and d, $H_{5'}$
B_2–B_1	8.45–8.7	m, $H_{3',5'}$	8.45	s, $H_{3'}$ and d, $H_{5'}$
B_2–B_2 and B_2–CPH	8.1	$H_{6'}$	8.1	$H_{6'}$
CPH–*CPH*	8.1	d, H_a	8.1	d, H_a
B_2–B_1	7.9	$H_{6'}$	7.9	$H_{6'}$
CPH–B_1 and *CPH*–B_2	7.9	d, H_a	7.9	d, H_a
CPH	7.0	dd, H_b	7.0	dd, H_b
	4.1	t, H_c	4.1	t, H_c
B $(CH_2)_{11}$			3.7	t, H_{11}
B_1–B_2	4.85	s, H_2	2.65	t, H_2
B_1–B_1	4.7	s, H_2	2.45	t, H_2
B_1–CPH	4.6	s, H_2	2.6	t, H_2

[a] B_1 and B_2 represent the aliphatic and the aromatic ends, respectively, of the asymmetric imide-containing unit. In the case of (TMA-gly:CPH) copolymers, the copolymer ratio was determined from the ratio of the integrated peak areas of either the methylene group at ca. 4.7 ppm or the aromatic protons of the imide-containing unit at ca. 8.5 ppm and the aromatic protons of the CPH unit at 4.1 ppm, respectively. In the case of (TMA-10:CPH) copolymers, the copolymer ratio was determined from the ratio of the integrated peak areas at 4.1 and 3.7 ppm, respectively (the italicized monomer represents the NMR-active one). TMA-*gly* possesses no more than one methylene group, which is reported separately for the various diads.

Table III
Observed Diad Probabilities in (TMA-gly:SA) Copolymers of Various Ratios

% TMA-gly	% SA	P_{SASA}	P_{SAB_1}	P_{SAB_2}
0.00	1.00	1.00	0.00	0.00
0.11	0.89	0.906	0.051	0.043
0.16	0.84	0.852	0.074	0.074
0.30	0.70	0.800	0.100	0.100
0.32	0.68	0.754	0.164	0.082
0.39	0.61	0.731	0.135	0.135
0.47	0.53	0.579	0.211	0.211
0.60	0.40	0.115	0.471	0.414

taining symmetric and asymmetric monomers of varying degrees of hydrophobicity—by ^{1}H NMR spectroscopy. The sequence distributions were determined by using the relative intensities of the corresponding diad sequences and the experimental results were compared to Bernoullian statistics. In addition, the glass transition temperatures were analyzed as a function of copolymer composition and sequence distribution and compared to theoretical calculations based on thermodynamic models.

Experimental Section

Materials. Trimellitic anhydride (TMA, Aldrich Chemical Co.) was recrystallized from a mixture of hot toluene and acetic anhydride. The amino acids used were glycine (Mallinckrodt), β-alanine, γ-aminobutyric acid (Sigma Chemical Co.), 5-aminovaleric acid, 6-aminocaproic acid, 11-aminoundecanoic acid, and 12-aminododecanoic acid (Aldrich). All the solvents (Gold Label, Aldrich) were used without further purification, unless otherwise specified. 1,3-Bis(*p*-carboxyphenoxy)hexane was prepared as previously reported.[19] The imide-containing diacids were prepared by condensation of equimolar amounts of amino acid and trimellitic anhydride.[1] All poly(anhydride-*co*-imides) were synthesized by melt polycondensation via their mixed anhydrides with acetic acid.[1]

Methods. The melting points were determined on a Fisher-Johns melting point apparatus. Infrared spectroscopy was obtained on a FTIR spectrophotometer (Mattson Instruments). The samples were either film cast in chloroform onto NaCl plates or pressed into KBr pellets. The molecular weights of all the polymer samples were determined on a GPC system (Perkin-Elmer, MA) consisting of the Series 10 pump, the LKB 214 rapid spectral detector at 254-nm wavelength, and the PE 3600 data station. The samples, dissolved in chloroform or a dimethylformamide–chloroform mixture, were eluted through a PL Gel column (Polymer Laboratories, PL-Gel, 30 cm × 7.5 mm, particles 5 mm, mixed bed) at a flow rate of 0.9 mL/min. The molecular weights of the polymers were determined relative to polystyrene standards (Polysciences). Elemental analysis was performed by Galbraith Laboratories (Knoxville, TN). ^{1}H and ^{13}C NMR spectra were obtained on a Varian 250- or 300-MHz and a Varian XL 400 spectrometer, respectively, using chloroform-d_1 or dimethyl-d_6 sulfoxide as a solvent and either tetramethylsilane (TMS, as an internal reference) or an external standard, respectively. Thermal analysis of the polymers was studied on the 7 Series thermal analysis system of Perkin-Elmer. An average sample weight of 2–10 mg was heated at consistent heating and cooling rates ranging from 1 to 20 °C/min.

Theoretical Models for T_g Calculation. The following three mathematical relations were used to calculate the glass transition temperatures. T_{gAA} (and T_{gBB}) and T_{gAB} represent the glass transition temperatures of the pure homopolymers and the strictly alternating copolymer, respectively. Equation 1 was proposed

$$T_g = N_{AA}T_{gAA} + N_{BB}T_{gBB} + (N_{AB} + N_{BA})T_{gAB} \qquad (1)$$

by Barton, based on the Gibbs–DiMarzio relation $T_{gAB} = N_A T_{gAA} + N_B T_{gBB}$; N_X and N_{XY} represent the molar fraction of the monomer X and of the diad XY, respectively.[9]

Johnston's approach (eq 2) was derived from the Fox equation: $1/T_g = (W_A/T_{gAA}) + (W_B/T_{gBB})$. W_X represents the weight fraction of the monomer X; P_{XY} represents the probability of finding the diad XY.[10]

$$1/T_g = W_A P_{AA}/T_{gAA} + W_B P_{BB}/T_{gBB} + (W_A P_{AB} + W_B P_{BA})/T_{gAB} \qquad (2)$$

A third relation was developed by Couchman, based on mixed-system entropy (expressed by glass transition temperatures and corresponding heat capacity increments).[11] Equation 3 represents its reduced form, assuming minimal variation of glass transition increments of heat capacity (f_{XY} represent the fraction of the diad XY).

$$\ln T_g = (f_{AA} \ln T_{gAA} + f_{BB} \ln T_{gBB} + f_{AB} \ln T_{gAB})/(f_{AA} + f_{BB} + f_{AB}) \qquad (3)$$

Results and Discussion

^{1}H NMR Analysis. Figure 1 summarizes the copolymers studied. Of the two monomers used, one was always symmetric (A) and the other asymmetric (B_1–B_2). The symmetric unit was either a hydrophilic polymethylene chain (sebacic acid, SA) or a more hydrophobic spacer containing aromatic moieties [1,3-bis(carboxyphenoxy)hexane, CPH]. The structure of the asymmetric monomer was varied by increasing the length of the polymethylene chain from one methylene (TMA-gly) to ten methylene groups (TMA-10). Typical ^{1}H NMR spectra of these copolymer systems are shown in Figure 2a–d. The molar fractions of the imide-containing monomer units incorporated into the polymer chain were determined from the corresponding relative intensities of the methylene groups and the aromatic protons. The monomer fractions of SA and CPH were determined from the relative intensities of the methylene groups or the aromatic protons, respectively. Due to the asymmetry of the trimellitimide-containing monomer units (TMA-gly or TMA-10), six diad sequences were expected to be present in a polymer backbone (A–A, A–B_1, A–B_2, B_1–B_1, B_1–B_2, and B_2–B_2; Figure 1) and were identified by ^{1}H NMR spectroscopy (Figure 2a–d). A total assignment of the peaks is given in Tables I and II. Due to partially overlapping peaks in some of the copolymers, the following assumptions were made during quantitative

Table IV
Observed Diad Probabilities and Degree of Randomness (*B*) in (TMA-gly:CPH) Copolymers of Various Ratios

% TMA-gly	% CPH	$P_{B_2B_2}$	$P_{B_2B_1}$	P_{B_2CPH}	P_{CPHCPH}	P_{CPHB_2}	P_{CPHB_1}	$P_{B_1B_1}$	$P_{B_1B_2}$	P_{B_1CPH}	*B*
0.000	1.000	0.000	0.000	0.000	1.000	0.000	0.000	0.000	0.000	0.000	
0.090	0.910	0.046	0.033	0.921	0.888	0.054	0.058	0.031	0.031	0.938	2.04
0.344	0.656	0.170	0.182	0.648	0.632	0.173	0.195	0.167	0.167	0.667	2.03
0.348	0.652	0.171	0.188	0.641	0.661	0.163	0.175	0.125	0.188	0.688	2.04
0.532	0.468	0.265	0.269	0.466	0.526	0.220	0.254	0.192	0.269	0.538	2.02
0.698	0.302	0.357	0.333	0.309	0.496	0.256	0.248	0.296	0.370	0.333	1.85

Table V
Observed Diad Probabilities and Degree of Randomness (*B*) in (TMA-10:SA) Copolymers of Various Ratios

% TMA-10	% SA	$P_{B_2B_2}$	P_{B_2SA}	$P_{B_2B_1}$	P_{SASA}	P_{SAB_1}	P_{SAB_2}	$P_{B_1B_1}$	$P_{B_1B_2}$	P_{B_1SA}	*B*
0.00	1.00	0.00	0.00	0.00	1.00	0.00	0.00	0.00	0.00	0.00	
0.13	0.87	0.14	0.66	0.20	0.91	0.07	0.02	0.08	0.08	0.85	1.87
0.33	0.67	0.17	0.60	0.23	0.69	0.14	0.17	0.24	0.24	0.53	1.91
0.44	0.56	0.23	0.45	0.32	0.64	0.20	0.16	0.27	0.27	0.45	1.86
0.51	0.49	0.27	0.37	0.37	0.58	0.23	0.19	0.31	0.31	0.37	1.84
0.53	0.47	0.26	0.38	0.36	0.53	0.22	0.25	0.34	0.34	0.32	1.87
0.62	0.38	0.28	0.38	0.34	0.41	0.23	0.37	0.37	0.37	0.25	1.95
0.72	0.28	0.28	0.33	0.39	0.34	0.28	0.38	0.38	0.38	0.24	2.00
0.82	0.18	0.33	0.21	0.46	0.24	0.32	0.44	0.43	0.43	0.14	2.00
0.87	0.13	0.36	0.14	0.50	0.21	0.40	0.39	0.44	0.44	0.12	1.99
1.00	0.00	0.42	0.00	0.58	0.00	0.00	0.00	0.50	0.50	0.00	1.08

Table VI
Observed Diad Probabilities and Degree of Randomness (*B*) in (TMA-10:CPH) Copolymers of Various Ratios

% TMA-10	%CPH	$P_{B_2B_2}$	$P_{B_2B_1}$	P_{B_2CPH}	P_{CPHCPH}	P_{CPHB_2}	P_{CPHB_1}	$P_{B_1B_1}$	$P_{B_1B_2}$	P_{B_1CPH}	*B*
0.00	1.00	0.000	0.000	0.000	1.000	0.000	0.000	0.000	0.000	0.000	
0.18	0.82	0.041	0.134	0.825	0.767	0.133	0.100	0.120	0.157	0.723	2.07
0.28	0.72	0.032	0.242	0.726	0.679	0.161	0.161	0.143	0.214	0.643	2.15
0.33	0.67	0.119	0.238	0.643	0.709	0.143	0.148	0.208	0.208	0.583	1.96
0.51	0.49	0.268	0.317	0.415	0.575	0.195	0.230	0.298	0.277	0.426	1.86
0.53	0.47	0.321	0.309	0.370	0.568	0.185	0.247	0.316	0.263	0.421	1.80
0.69	0.31	0.263	0.421	0.316	0.403	0.299	0.299	0.364	0.364	0.273	1.97
1.00	0.00	0.421	0.579	0.000	0.000	0.000	0.000	0.500	0.500	0.000	

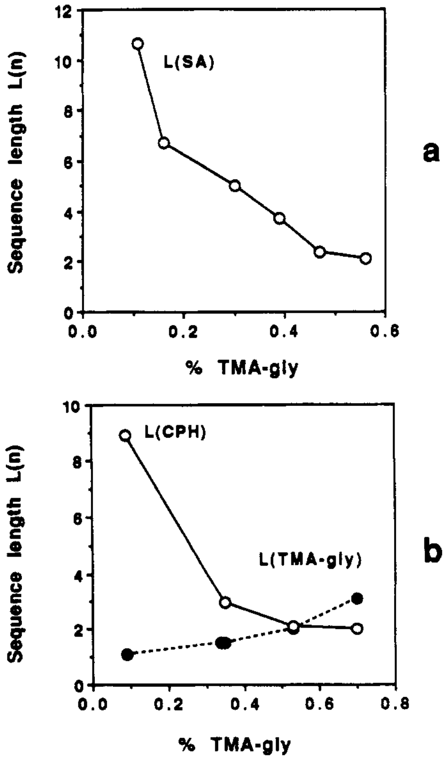

Figure 3. Sequence lengths in (a) (TMA-gly:SA) and (b) (TMA-gly:CPH) copolymers.

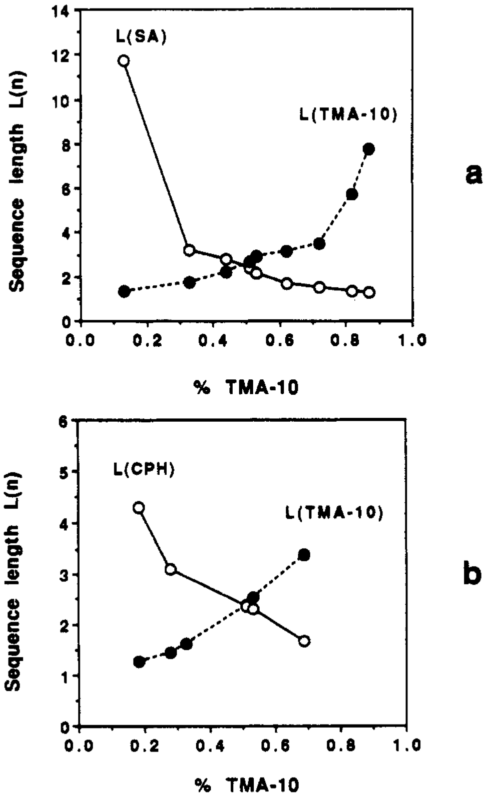

Figure 4. Sequence lengths in (a) (TMA-10:SA) and (b) (TMA-10:CPH) copolymers.

analysis. The aromatic peaks of the various (TMA-10:SA) copolymers were resolved by using the integrated peak ratios of the diad sequences determined for the (TMA-10) homopolymer [this assumption was verified with the (TMA-10:CPH) copolymers, where the same sequence distribution was obtained by using either the integrated peak ratios only (identified by ^{1}H NMR) or in combination with the determined reactivity ratio for the asymmetric

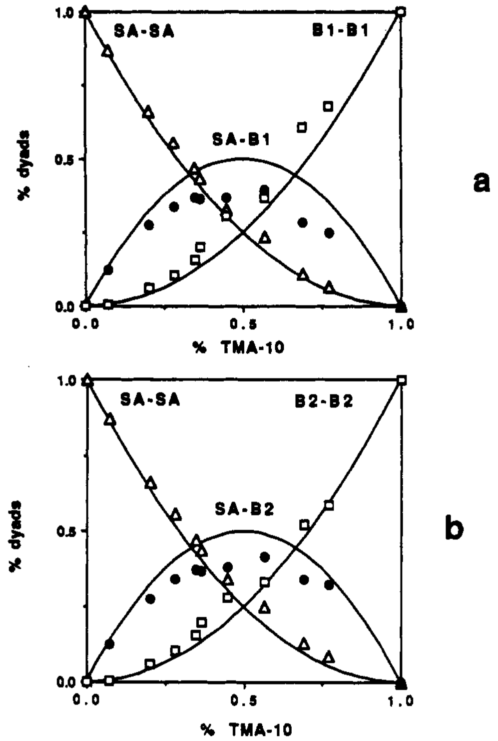

Figure 5. Diad distribution of (TMA-10:SA) copolymers (a) between B_1 and SA and (b) between B_2 and SA. SA–SA (Δ), SA–B_1 and SA–B_2 (●), and B_1–B_1 and B_2–B_2 (□) represent the observed relative integrated intensities of the corresponding peaks. Solid lines represent ideal Bernoullian distribution.

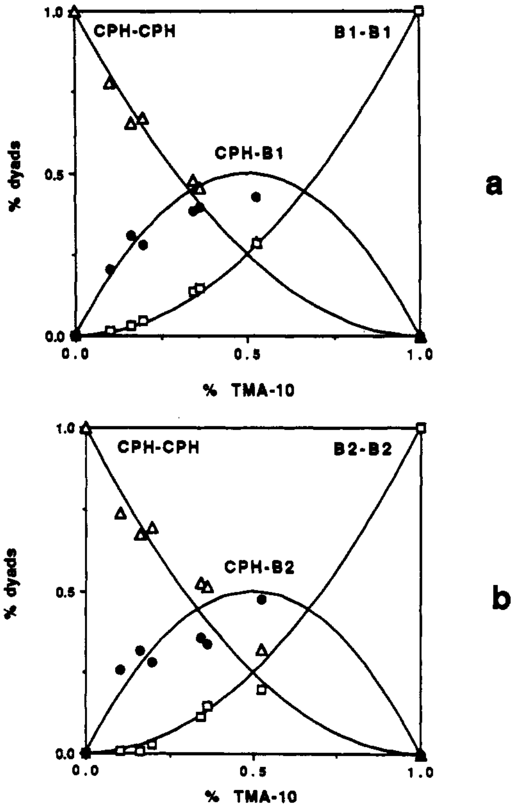

Figure 6. Diad distribution of (TMA-10:CPH) copolymers, (a) between B_1 and CPH and (b) between B_2 and CPH. CPH–CPH (Δ), B_1–CPH and B_2–CPH (●), and B_1–B_1 and B_2–B_2 (□) represent the observed relative integrated intensities of the corresponding peaks. Solid lines represent ideal Bernoullian distribution.

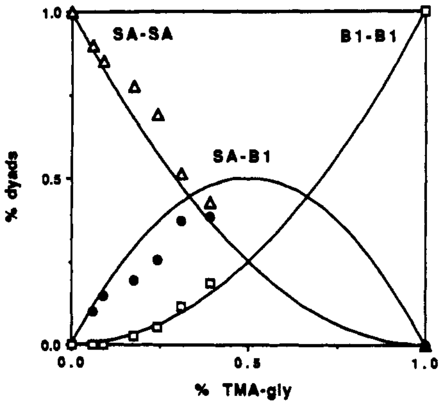

Figure 7. Diad distribution of (TMA-gly:SA) copolymers. SA–SA (Δ), SA–B_1 (●), and B_1–B_1 (□) represent the observed relative integrated intensities of the corresponding peaks. Solid lines represent ideal Bernoullian distribution.

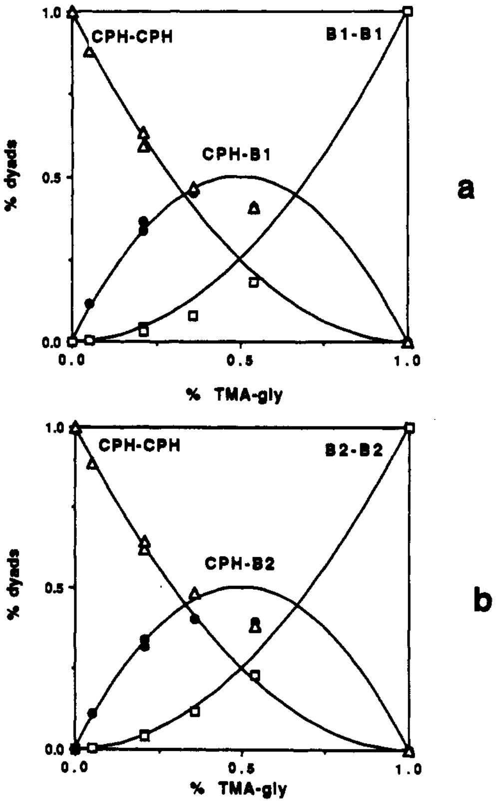

Figure 8. Diad distribution of (TMA-gly:CPH) copolymers, (a) between B_1 and CPH and (b) between B_2 and CPH. CPH–CPH (Δ), B_1–CPH and B_2–CPH (●), and B_1–B_1 and B_2–B_2 (□) represent the observed relative integrated intensities of the corresponding peaks. Solid lines represent ideal Bernoullian distribution.

TMA-10 monomer]. In addition, since the methylene groups of both the TMA-10 and the SA monomer experienced the same shift, the assumption was made (based on the structural similarity of B_1 and SA), that the formation of either a SA–B_1 or SA–SA diad was predominantly a function of the molar fraction of either the B_1 or SA unit, respectively. The analysis of the (TMA-gly: SA) copolymers was partially restricted by low solubility and low molecular weights of the copolymers as the SA content decreased.

Based on the relative intensities of the integrated peaks ($p_{X\text{-}Y}$), the probabilities of finding a particular diad sequence along the polymer chain (P_{XY}) were then calculated by using eq 4 (the polymer systems were treated

$$P_{AB_1} = 0.5p_{A\text{-}B_1}/(0.5p_{A\text{-}B_1} + 0.5p_{A\text{-}B_2} + p_{A\text{-}A}) \quad (4)$$

as terpolymers of the monomers A, B_1, and B_2, with B_1

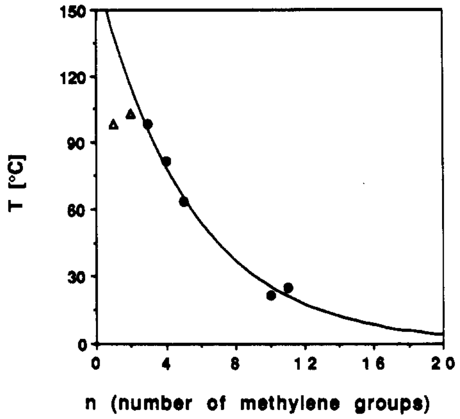

Figure 9. T_g's of homopolymers with increasing polymethylene chain length n.

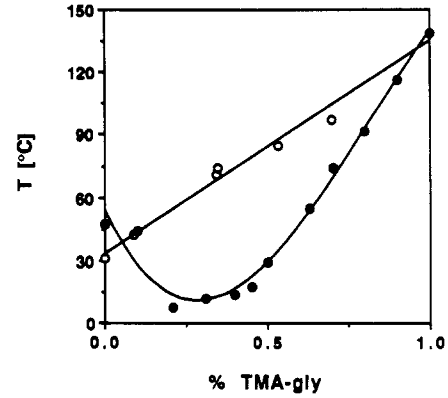

Figure 10. T_g's of TMA-gly copolymerized with SA (●) or CPH (○) in various ratios.

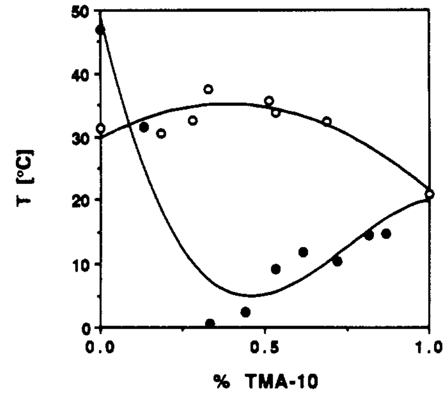

Figure 11. T_g's of TMA-10 copolymerized with SA (●) or CPH (○) in various ratios.

and B_2 having the same molar fraction) (Tables III–VI). P_{AA}, P_{AB_2}, $P_{B_1B_1}$, $P_{B_1B_2}$, and $P_{B_2B_2}$ were calculated in an analogous manner. In addition, the average sequence length (L_n) and the degree of randomness (B), which is defined in a terpolymer by the sum of the various diad sequences containing different monomer units, was determined from eqs 5 and 6, respectively (Figures 3 and 4;

$$L_A = 1/(P_{AB_1} + P_{AB_2}) \qquad (5)$$

$$B = P_{AB_1} + P_{B_1A} + P_{AB_2} + P_{B_2A} + P_{B_1B_2} + P_{B_2B_1} \qquad (6)$$

Tables III–VI). B equals 2 in the case of a random terpolymer [following Bernoulli statistics (since $P_{AB_1} = P_{B_1A}$, $P_{AB_2} = P_{B_2A}$, and $P_{B_1B_2} = P_{B_2B_1}$)]. As shown in Tables III–VI, the calculated values for all the copolymer systems are close to the corresponding values of a Bernoullian sequence distribution. This is also illustrated in Figures 5–8, which show the observed diad ratios of either B_1 or B_2 (of the imide-containing monomer) with SA and CPH, respectively, as a function of the normalized molar fraction of one monomer unit. The solid curves in the figures represent ideal random (Bernoullian) distribution of the monomers. Furthermore, the average sequence lengths of either monomer unit in the four copolymer systems of equimolar composition approach the theoretical value of 2, as expected for a Bernoullian distribution (Figures 3 and 4). These results suggest that, for the reported systems, poly(anhydride) formation by melt polycondensation was fairly independent of the nature of the repeating units and always adopted a near-random configuration.

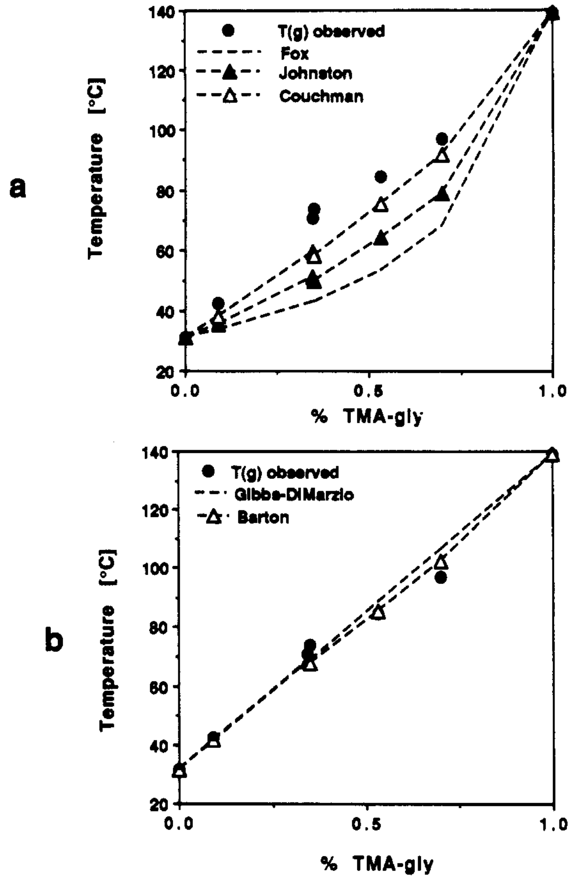

Figure 12. T_g's of (TMA-gly:CPH) copolymers as observed by DSC or calculated with (a) the Fox, Johnston, and Couchman relation or (b) the Gibbs–DiMarzio and the Barton relation.

Knowing the sequential structure of a copolymer allows us to analyze many properties of copolymer systems (e.g., thermal behavior, degree of crystallinity) that depend on the sequence distribution of the monomers, i.e., on the molecular interactions between adjacent monomer units. Increasing interest has specifically concentrated on relating the molecular structure and sequence distribution of a copolymer (as determined by ^1H NMR spectroscopy) to its glass transition behavior. Several reports have shown that copolymer glass transition temperatures can generally be accurately predicted if the sequence distribution is known.[9-11]

Glass Transition Temperature Analysis of Poly(anhydride-*co*-imides). As opposed to the observed reactivities (which resulted in nearly random distributions for all the reported copolymers), the glass transition behavior was very sensitive toward the chemical nature of the monomer. The homopolymers of the imide-containing

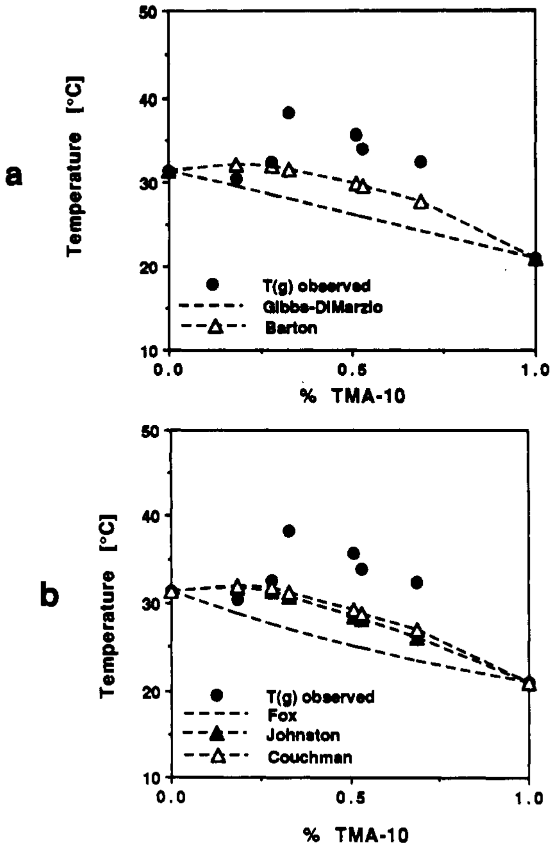

Figure 13. T_g's of (TMA-10:CPH) copolymers as observed by DSC or calculated with (a) the Gibbs–DiMarzio and the Barton relation or (b) the Fox, Johnston, and Couchman relation.

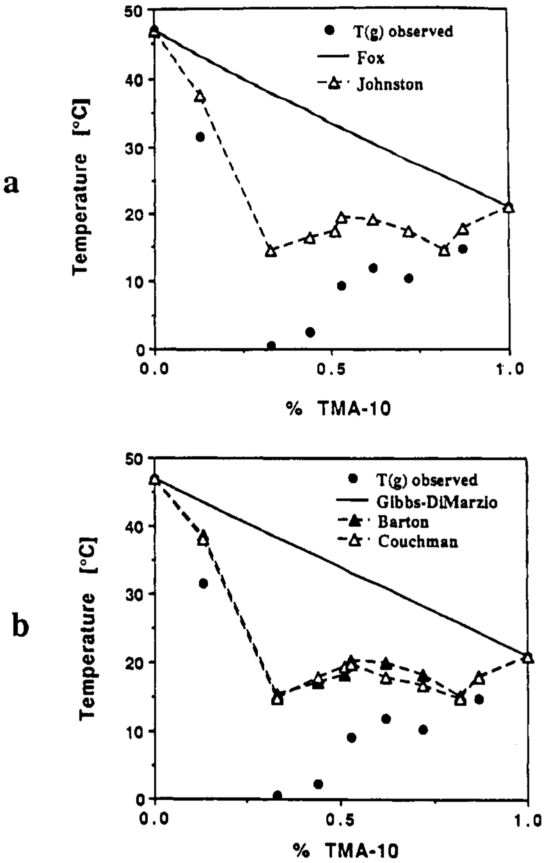

Figure 14. T_g's of (TMA-10:SA) copolymers as observed by DSC or calculated with (a) the Fox, and Johnston relation or (b) the Gibbs–DiMarzio, Barton, and Couchman relation.

monomers with polymethylene chains of various length were used to determine the effect of aliphatic spacers on the glass transition temperatures (i.e., without the sequence distribution effects). The glass transition behavior of these homopolymers is illustrated in Figure 9. All of these homopolymers displayed T_g's that decreased with increasing chain length as a result of higher flexibility and increasing molecular motion [corresponding to previously reported poly(ester imides) of analogous structure[20]]. A theoretical value of 139 °C (as compared to the experimentally obtained value of 98 °C) was obtained for the (TMA-gly) homopolymer after extrapolation of the T_g's of the homopolymers containing spacers ranging fromn 3 to 11 methylene groups, using an exponential decay function [$y = 167.97 \times 10 \exp(-0.0817x)$] as a least-squares progression fit (Figure 9). The experimentally observed low T_g of the (TMA-gly) homopolymer was probably due to its low molecular weight (the lower the molecular weight of a polymer, the more free chain ends are present, which are able to move around more easily, therefore lowering the T_g[6]).

A substantially different T_g behavior was observed in the case of copolymers as a function of the chemical nature of the incorporated monomers. Copolymerization of both imide-containing monomers with an aliphatic chain (SA) showed a large negative deviation of their glass transition temperatures from linearity. A minimal T_g was observed in both copolymer systems—(TMA-gly:SA) and (TMA-10:SA)—at approximately 30% SA (Figures 10 and 11). Increasing T_g's were observed as the SA content increased, which was due to the high crystallizability of the SA chains, limiting the amorphous content of these copolymers. A totally different behavior was observed if the aliphatic SA was replaced by the more hydrophobic and aromatic CPH. In the case of the (TMA-gly:CPH) copolymers a linear relationship was observed, which suggested some structural compatibility of these two fairly rigid, aromatic monomers (Figure 10). Introducing a long polymethylene chain into the imide-containing monomer reflected on the glass transition behavior, such that a slight positive deviation from linearity was observed for the (TMA-10:CPH) copolymers (Figure 11).

The experimental T_g's of TMA-10 copolymerized with either SA or CPH as well as the (TMA-gly:CPH) copolymers were then compared with the predicted values by using either simple additive relations only or the sequence distribution dependent theories (eqs 1–3). To apply the latter ones, it was necessary to determine the T_g of a strictly alternating copolymer. In the case of the (TMA-10:SA) copolymers, the value of a strictly alternating copolymer was approximated from the homopolymer containing a polymethylene chain of the corresponding length (e.g., TMA-20). The obtained value of 3.5 °C corresponded nicely to the experimentally observed value of 5 °C of the synthesized copolymer (TMA-10:SA) (50:50), which is not strictly alternating, but contains alternating pairs of both TMA-10 and SA units ...-AA-BB-AA-BB-AA-... (as determined by ^{1}H NMR). On the basis of this observation the values for strictly alternating copolymers in the case of (TMA-10:CPH) and (TMA-gly:CPH) copolymers—which also showed a random distribution according to ^{1}H NMR analysis—were estimated by the experimentally observed values of the corresponding equimolar copolymers and were found to be 34.6 °C in the former and 84.1 °C in the latter case. Figure 12 shows that both the additive relations by Fox and Gibbs–DiMarzio as well as their extended sequence distribution dependent versions by Johnston, Barton, and Couchman were able to describe the linear relationship found in the case of (TMA-gly:CPH) copolymers. The slight positive deviation observed for the (TMA-10:CPH) copolymers showed, in general, a better correlation with the predicted values from the sequence distribution dependent equations (Figure 13). The potential of these relations however is most evident in the case of the (TMA-10:SA) copolymers, where the sequence distribution dependent theories were able to approximate the large negative deviation as opposed to the additive relations (Figure 14).

Acknowledgment. We thank Melissa Lucarelli for her laboratory assistance. This study was supported by NIH Grant GM 26698 and a gift from NOVA Pharmaceuticals.

References and Notes

(1) Staubli, A.; Ron, E.; Langer, R. *J. Am. Chem. Soc.* **1990**, *112*, 4419.

(2) Staubli, A.; Mathiowitz, E.; Langer, R. *Macromolecules*, in press.

(3) Bovey, F. A. *Nuclear Magnetic Resonance Spectroscopy*, 2nd ed.; Academic Press: New York, 1987.

(4) Murano, M. *Polym. J.* **1970**, *1*, 660.

(5) Hill, D. J. T.; O'Donnell, J. H.; O'Sullivan, P. W. *Macromolecules* **1982**, *15*, 960.

(6) Eisenberg, A. In *Physical Properties of Polymers*; Mark, J. E., Eisenberg, A., Grassley, W. W., Mandelkern, L., Koenig, J. L., Eds.; American Chemical Society: Washington, DC, 1984; p 55.

(7) Gibbs, J. H.; DiMarzio, E. A. *J. Polym. Sci., Part A-1* **1963**, 1417.

(8) Fox, T. G. *Bull. Am. Phys. Soc.* **1956**, *1*, 123.

(9) Barton, J. M. *J. Polym. Sci. C* **1970**, *30*, 573.

(10) Johnston, N. W. *J. Macromol. Sci., Rev. Macromol. Chem.* **1976**, *C14*, 215.

(11) (a) Couchman, P. R. *Macromolecules* **1982**, *15*, 770. (b) Couchman, P. R. *Nature* **1982**, *298*, 729. (c) Couchman, P. R. *Macromolecules* **1978**, *11*, 1157.

(12) Fox, T. G.; Flory, P. J. *J. Appl. Phys.* **1950**, *21*, 581.

(13) Gordon, M.; Taylor, J. S. *J. Appl. Chem.* **1952**, *2*, 493.

(14) Kelley, F. N.; Bueche, F. *J. Polym. Sci., Part A-1* **1963**, 1417.

(15) *Structure and Mobility in Molecular and Atomic Glasses*; O'Reilly, J. M., Goldstein, M., Eds.; *Ann. N.Y. Acad. Sci.* **1981**, 371.

(16) Uematsu, I.; Honda, K. *Rep. Prog. Polym. Phys. Jpn.* **1965**, *8*, 111.

(17) Hirooka, M.; Kato, T. *J. Polym. Sci., Polym. Lett. Ed.* **1971**, *9*, 199.

(18) Furukawa, J. *J. Polym. Sci., Polym. Symp.* **1975**, *51*, 105.

(19) Conix, A. *Macromol. Synth.* **1966**, *2*, 95.

(20) Kricheldorf, H. R.; Pakull, R.; Buchner, S. *J. Polym. Sci., Polym. Chem.* **1989**, *27*, 431.